



Irpex lacteus polysaccharide exhibits therapeutic potential for ovarian fibrosis in PCOS rats via the TGF- β 1/smad pathway

Yan-Yuan Zhou^{a,1}, Ya-Qi Wu^{a,1}, Chao-Jie Chong^{a,1}, Shu-Mei Zhong^b,
Zi-Xian Wang^b, Xiao-Hui Qin^a, Zhi-Qiang Liu^a, Jun-Yang Liu^b, Jia-Le Song^{b,c,d,e,*}

^a Department of Pharmacy, School of Pharmacy, Guilin Medical University, Guilin, 541199, China

^b Department of Nutrition and Food Hygiene, School of Public Health, Guilin Medical University, Guilin, 541199, China

^c Department of Clinical Nutrition, Second Hospital Affiliated to Guilin Medical University, Guilin, 541100, China

^d Guangxi Key Laboratory of Environmental Exposomics and Entire Lifecycle Health, Guilin Medical University, Guilin, 541199, China

^e South Asia Branch of National Engineering Research Center of Dairy Health for Maternal and Child Health, Guilin University of Technology, Guilin, 541004, China

ARTICLE INFO

Keywords:

Irpex lacteus polysaccharides
Polycystic ovary syndrome
TGF- β 1/Smad
Oxidative stress
Metabolic disorders

ABSTRACT

Polycystic ovarian syndrome (PCOS) is one of the commonest endocrinopathies in childbearing women. The research was conducted to assess the impact of *Irpex lacteus* polysaccharide (ILP, 1000 mg/kg) on the letrozole (1 mg/kg)-induced PCOS model in female rats. Metformin (Met, 265 mg/kg) as the positive control. The study suggested that ILP restored the estrous cycle in rats with PCOS as well as lowered relative ovarian weight and body weight, in comparison to normal. Rats with PCOS showed improvement in ovarian structure and fibrosis when given ILP. ILP decreased the testosterone (T), low-density lipoprotein cholesterol (LDL-C), triglyceride (TG), total cholesterol (TC), luteinizing hormone (LH), homeostasis model assessment-insulin resistance (HOMA-IR), fasting blood glucose (FBG), and insulin (INS) levels and elevated the follicle-stimulating hormone (FSH) and estrogen (E2) levels in PCOS rats. In addition, ILP increased the content of superoxide dismutase (SOD) in serum and the antioxidant enzymes (*Prdx3*, *Sod1*, *Gsr*, *Gsta4*, *Mgst1*, *Gpx3*, *Sod2* and *Cat*) expression levels in the ovaries and decreased the serum expression of malondialdehyde (MDA). In addition, ILP treatment slowed down the process of the fibrosis-associated TGF- β 1/Smad pathway and downregulated α -smooth muscle actin (α -SMA) and connective tissue growth factor (CTGF) levels in PCOS rats ovaries. According to these findings, ILP may be able to treat letrozole-induced PCOS in rats by ameliorating metabolic disturbances, sex hormone levels, oxidative stress, and ovarian fibrosis.

1. Introduction

Polycystic ovary syndrome (PCOS) is a prevalent gynecologic endocrine condition that is an important contributor to anovulatory infertility in women of fertile age. PCOS has a global incidence of 6%–10% [1], with China having a frequency of 5.6% [2]. Obesity,

* Corresponding author. Department of Nutrition and Food Hygiene, School of Public Health, Guilin Medical University, Guilin, 541199, China.
E-mail addresses: zyy@glmc.edu.cn (Y.-Y. Zhou), wuyaqi@stu.glmc.edu.cn (Y.-Q. Wu), chongchaojie@stu.glmc.edu.cn (C.-J. Chong), zhongshumei@stu.glmc.edu.cn (S.-M. Zhong), wangzixian@stu.glmc.edu.cn (Z.-X. Wang), qinxiaohui@stu.glmc.edu.cn (X.-H. Qin), liuzhiqiang@stu.glmc.edu.cn (Z.-Q. Liu), liujunyang@stu.glmc.edu.cn (J.-Y. Liu), Songjiale@glmc.edu.cn (J.-L. Song).

¹ These authors contributed equally to this work.

<https://doi.org/10.1016/j.heliyon.2023.e18741>

Received 14 October 2022; Received in revised form 10 July 2023; Accepted 26 July 2023

Available online 27 July 2023

2405-8440/© 2023 Published by Elsevier Ltd.

This is an open access article under the CC BY-NC-ND license

(<http://creativecommons.org/licenses/by-nc-nd/4.0/>).

hirsutism, acne, diabetes, impaired glucose metabolism and insulin resistance (IR) are also in connection with PCOS [3]. Cardiovascular disease, endometrial cancer, and nonalcoholic fatty liver are more likely to occur [4,5], the precise causes of this complex of metabolic dysfunctions are still unknown. Published studies have suggested a possible association with abnormal hypothalamic-pituitary-ovarian axis (HPOA) function [6,7]. A decapeptide, gonadotrophin-releasing hormone (GnRH), plays an important role in controlling HPOA axis expression. The sub-hypothalamic nucleus releases GnRH in a pulsatile manner, which induces the release of follicle-stimulating hormone (FSH) and luteinizing hormone (LH) from the anterior pituitary. FSH promotes the development of ovarian follicles, while LH controls ovulation and the production of luteal cells androgens. Boosted hypothalamic GnRH pulse frequency leads to the preferential secretion of LH by the pituitary gland, elevated levels of LH stimulate androgen synthesis in the ovary, and a relative FSH deficiency can result in follicular arrests, polycystic ovarian patterns, and oligoovulation or anovulation [8].

Fibrosis frequently takes place in the development of a chronic disease that has progressed to an advanced stage. In the absence of effective treatment, it may progress to severe scarring, which may exacerbate organic disease and potentially result in a functional decline or organ failure [9]. Fibrosis of the ovary is a major contributor to ovarian hypofunction and ovarian function decline. The ovaries of PCOS patients express abnormally high concentrations of transforming growth factor β 1 (TGF- β 1). TGF- β 1 has the ability to both promote the generation of extracellular matrix (ECM) proteins in mesenchymal cells and boost the creation of protease inhibitors which impede the enzymatic breakdown of the ECM. Finally, excessive ECM accumulation in PCOS patients' ovaries promotes ovarian interstitial fibrosis, endangering women's reproductive health and quality of life [10].

TGF- β 1, one of the transforming growth factors, is the most important profibrotic factor, and the Smad protein is a primary intracellular effector of TGF- β 1 signaling that causes fibrogenic effects [11]. TGF- β 1 acts biologically by promoting downstream mediator activation such as Smad2 and Smad3, whereas Smad7 is the negative feedback regulator. TGF- β 1 interacts with transforming growth factor β receptor II (TGF- β RII). TGF- β RII phosphoric transforming growth factor β receptor I (TGF- β RI), which phosphoric Smad2/Smad3 and forms a heterotrimeric complex with Smad4, translocated into the nucleus, acts on TGF- β 1 target genes and regulates target gene transcription [4].

At present, PCOS is treated by adjusting the menstrual cycle, promoting conception, reducing the level of androgens in the body, increasing the sensitivity of the body to insulin, and in severe cases, surgical treatment and assisted reproduction techniques are used. Ovulation rates were significantly higher in patients treated with Western medicine alone, but some patients still experienced unavoidable miscarriages and reduced pregnancy rates [12], with side effects such as abdominal distention, visual disturbances, headache and nausea [13]. Metformin (Met) is one of the primary methods of ovulation induction for PCOS patients, which increases tissue cell sensitivity to insulin [14]. However, it can also cause diarrhea, and gastrointestinal disturbances, along with a multi-pregnancy and ovarian hyperstimulation risk, which may lead to an unsatisfactory outcome of the treatment [15,16].

In recent years, traditional Chinese medicinal and food plants have shown good therapeutic efficacy in the treatment of PCOS [17]. *Dendrobium officinale* polysaccharide [18], berberine [19], and puerarin [20] have performed well in the treatment of PCOS when it comes to the regulation of endocrine and metabolic disorders. Medicinal fungi are an important part of Chinese traditional medicine and they have various biological activities, such as antitumor, immunomodulatory, antioxidant, free radical scavenging, cardioprotective, and antiviral effects [21,22]. Polysaccharides are naturally occurring macromolecules found in plants, animals, algae, and microorganisms. Natural polysaccharides are abundant and have low toxicity and multiple bioactive like immunomodulatory, antioxidant, hypoglycaemic, anti-tumor and anti-fibrotic [23]. *Irpex lacteus*, a medicinal fungus, has polysaccharides as its significant bioactive components [24]. *Irpex lacteus* polysaccharide (ILP) has been shown to have an ameliorative effect on hepatic oxidative stress (OS) [25].

2. Materials and methods

2.1. Experimental materials

Irpex lacteus polysaccharide (ILP, purity >98%) was acquired by Xi'an Ruidi Biotechnology Co., Ltd. (Xi'an, China). Letrozole (CAS: 112809-51-5) was purchased from Shanghai Yuanye Biotechnology Co., Ltd. (Shanghai, China). Carboxymethyl cellulose (CMC, CAS:9004-32-4) was bought by Xilong Science Co., Ltd. (Shantou, China). Papanicolaou staining, Masson's trichrome reagents, and Hematoxylin and eosin (H&E) has been provided by Solarbio Technology Co., Ltd. (Beijing, China). Metformin (Met, CAS: 1115-70-4, purity >99%) has been acquired by Jiuding Chemical Technology Co., Ltd. (Shanghai, China). The bicinchoninic acid (BCA) assay kits, anti-TGF- β 1 (AF0297), anti-CTGF (AF6582), anti-TGF- β RI (AF8148), anti-p-Smad3 (AF1759), anti-Smad3 (AF1501), anti-p-Smad2 (AF2545), anti-Smad2 (AF1300), anti-Smad7 (AF8004), anti-Smad4 (AF1291) and were provided by Beyotime Biotechnology Co., Ltd. (Shanghai, China). Anti- α -SMA (GB11044) was provided by Servicebio Biotechnology Co., Ltd. (Wuhan, China). Anti-GAPDH (AF7021) has been purchased by Affinity Biological Research Center Co., Ltd. (Jiangsu, China). Low-density lipoprotein cholesterol (LDL-C, ADS-F-QT031), high-density lipoprotein cholesterol (HDL-C, ADS-F-QT033), total cholesterol (TC, ADS-W-ZF014), triglyceride (TG, ADS-W-ZF013), superoxide dismutase (SOD, ADS-W-KY011), and malondialdehyde (MDA, ADS-W-YH002) has been purchased by Aidisheng Biological Technology Co., Ltd. (Jiangsu, China). Testosterone (T, MM-0577R), insulin (INS, MM-0587R1), luteinizing hormone (LH, MM-0624R1), estrogen (E2, MM-0575R1), follicle-stimulating hormone (FSH, MM-70867R1) and ELISA kits have been provided by Jiangsu Meimian Industrial Co., Ltd. (Jiangsu, China).

2.2. The evaluation of ILP for fourier transform infrared spectroscopy (FTIR)

To verify the polysaccharide structure of ILP, it was assayed by FTIR. Weighed 150 mg of KBr and 4 mg of ILP into a mortar and mixed [26], ground to a smooth powder and pressed into thin slices using a tablet press. The IRPrestige-21 FTIR spectrometer (Shimadzu, Tokyo, Japan), was used to measure the absorbance in the 400 cm^{-1} to 4000 cm^{-1} range.

2.3. High-performance liquid chromatography (HPLC) for determining ILP

A sensitive Agilent 1260 HPLC system (Agilent Technologies Inc., Santa Clara, CA, USA) with Xbridge C18 Columns (Waters Corporation, Shanghai, China, $5\text{ }\mu\text{m}$, $4.6 \times 150\text{ mm}$) was employed to determine the monosaccharide composition by pre-column derivatization using 1-phenyl-3-methyl-5-pyrazolone (PMP) [27]. Standardization of monosaccharides with D-arabinose (Ara), fructose (Fru), D-xylose (Xyl), rhamnose (Rha), glucose (Glc), D-glucuronic acid (Glc-A), D-galacturonic acid (Gal-A), D-galactose (Gal), L-fucose (Fuc) and mannose (Man). Both ILP and the monosaccharides were derived from PMP. The mobile phase was a mixture of 83% phosphate-buffered saline (PBS, 0.02 M, pH 6.7) and 17% acetonitrile solution. The injection volume is 20 μL and the flow rate is regulated at 1 mL/min. At 30 °C, the separation outcome was measured at 245 nm.

2.4. Animal experimental design

Thirty-two female Sprague–Dawley (SD) rats (6 weeks old, 180–220 g) were provided by Hunan Silaike Jingda Laboratory Animal Co., Ltd. (Changsha, China). An environment of standard conditions ($25 \pm 1\text{ }^\circ\text{C}$) was maintained for all rats with 12:12 h light/dark cycles. There was no restriction on access to water and food for any of the rats. Following 7 days of acclimating, the animals were randomized into 4 groups: Normal, PCOS, Met, and ILP groups. The gavage method was utilized for all animals, with the normal group receiving an equal volume of saline; the PCOS group receiving letrozole (1 mg/kg, dissolved in 1% CMC); the Met group were given both letrozole and Met (265 mg/kg) [28]; and the ILP group were given both letrozole and ILP (1000 mg/kg) [25]. Throughout the 21-day trial phase, rats were weighed every 3 days. Approval for this research was obtained from the Institutional Animal Care and Use Committee of Guilin Medical University (IACUC-GMU, approval number: GLMC-201803009).

2.5. Papanicolaou staining

All rats were examined for vaginal smears to assess their estrous cycle daily during the last 10 days. Rats were handled with a sterile cotton swab soaked in saline which was smeared clockwise on their vaginal walls. The swab was then smeared on a slide in the same direction. After drying at room temperature, they were fixed in 95% ethanol for 15 min and subsequently processed for Papanicolaou staining [29].

2.6. Serum and tissue sampling

The fasting blood glucose (FBG) level was measured after 12 h of overnight fasting. Blood, ovarian and periuterine adipocytes were collected after the rats were sacrificed. Following 30 min at room temperature, the blood was centrifuged for 15 min at 3000 rpm. Before analysis, serum and right ovaries were kept at $-80\text{ }^\circ\text{C}$.

2.7. Histopathologic observation

Cleaned the left ovaries and periuterine adipocytes in saline and placed them in 10% formaldehyde for fixation. After embedding and sectioning ($4\text{ }\mu\text{m}$), take the tissue samples to H&E and Masson's reagents stained for histopathological examination. The morphological structure and degree of fibrosis of the ovaries were observed by a Leica DM4B microscope (Leica Microsystems Inc., Buffalo Grove, IL, USA). Adipocyte areas and the results of the Masson experiment were examined using the ImageJ software (NIH Image, Bethesda, MD, USA).

2.8. Biochemical assay for serum hormones

An enzyme-linked immunosorbent assay (ELISA) was used to measure the hormone levels of FSH, E2, LH, T and fasting INS in the serum. The ratio of LH/FSH and homeostasis model assessment-insulin resistance (HOMA-IR) level were calculated ($\text{HOMA-IR} = \text{FBG (mmol/L)} \times \text{fasting INS (mU/L)} / 22.5$) [30]. Serum levels of LDL-C, TC, TG, MDA, SOD and HDL-C were measured using biochemical kits.

2.9. Western blot analysis

The frozen ovaries were cut into 30 mg samples and washed with saline. They were blotted dry with filter paper and RIPA lysis solution was added, followed by homogenization in a tissue grinder. After 1 h on ice, the homogenate is centrifuged at 14,000 rpm for 15 min at $4\text{ }^\circ\text{C}$. After the aspiration of the upper clear layer, its protein concentration was measured by the BCA kit and adjusted to unity. Separate the protein with a 10%–12% SDS-PAGE and then transmitted it to PVDF membranes with a thickness of $0.45\text{ }\mu\text{m}$.

Blocking the membranes with 5% skimmed milk before being treated with an overnight period at 4 °C with the appropriate primary antibodies: TGF- β 1 (1: 700), TGF- β RI (1: 1000), Smad2 (1: 1500), p-Smad2 (1: 1500), Smad3 (1: 1500), p-Smad3 (1: 1000), Smad4 (1: 1500), Smad7 (1: 1000), CTGF (1: 1500), α -SMA (1: 7000), and GAPDH (1: 10,000). The next day, the PVDF membrane was conjugated for 1 h with horseradish peroxidase (HRP)-labeled goat anti-rabbit IgG secondary antibody (1:20,000, EM35111-01, Beijing Emarbio Science & Technology Co. Ltd., Beijing, China) at room temperature. The blots were detected by the Fluor Chem system (Protein Simple, San Jose, CA, USA). Using ImageJ software (NIH Image, Bethesda, MD, USA) to analyze the optical density of the protein bands.

2.10. Immunohistochemical (IHC) staining

Sections (4 μ m) [31] were subjected to an oven temperature of 65 °C for a duration of 30 min and then dewaxed in xylene. A solution of EDTA antigen retrieval(pH 9.0) was used to retrieve antigens for 20 min after rehydration (with alcohol) of the slides. The tissue sections were subjected to blocking using 10% goat serum at room temperature for a duration of 30 min, followed by incubation with primary antibodies for immunohistochemistry of Smad2, Smad3, Smad4, Smad7 and TGF- β 1. HRP-conjugated goat anti-rabbit IgG secondary antibody was combined with the sections at a temperature of 37 °C for a duration of 30 min and then reacted with streptavidin. Next, DAB and hematoxylin staining, dehydrated in gradient alcohol and sealed with neutral resin was done. The expression of the above proteins was observed in the ovarian tissue by a Leica DM4B microscope (Leica Microsystems Inc., Buffalo Grove, IL, USA). Positive expression areas were analyzed with ImageJ software (NIH Image, Bethesda, MD, USA).

2.11. qRT-PCR assay

TRIzol reagent (Tiangen Biotech Co., Ltd., Beijing, China) was used to obtain ovarian RNA. The mRNA levels of *Sod1*, *Gpx3*, *Sod2*, *Gsta4*, *Cat*, *Prdx3*, *Gsr*, and *Mgst1* were measured by a Quant Studio 6 Flex Real-Time PCR System (Thermo Fisher Scientific, Waltham, MA, USA) using an SYBR Green quantitative PCR kit (Tiangen Biotech Co., Ltd., Beijing, China). Based on the $2^{-\Delta\Delta C_t}$ method calculated relative mRNA content and regard *GAPDH* as a reference. Table 1 provides the primer sequences used in the reactions.

2.12. Statistical analysis

Statistics are processed with SPSS 26.0 software and shown as mean \pm standard deviation (SD). One-way analysis of variance (ANOVA) and a Bonferroni test were applied to assay the statistical significance of the differences between groups. Statistically significant was defined as a *p-value* < 0.05. Graphs were plotted using GraphPad Prism 8.4.2. Positive expression area for Masson staining, adipocyte area, Western blot protein expression area and immunohistochemistry positive expression area were all measured using Image J.

3. Results

3.1. FTIR analyses of ILP

A stretching vibration of the O–H group at approximately 3375 cm^{-1} and a stretching and bending vibration of the C–H group at approximately 2921 cm^{-1} have been identified, respectively. The uronic acid-specific absorption peaks, which were seen at around 1643 cm^{-1} and 1412 cm^{-1} , were in correspondence with carboxyl and carbonyl groups, respectively [32]. Peaks at 1361 cm^{-1} and 1139 cm^{-1} show that sulfate groups should be present [33]. The peaks at 1016 cm^{-1} and 752 cm^{-1} are characteristic bands from a galactose backbone. Moreover, there is an absorption peak between 1000 and 1200 cm^{-1} resulting from the overlap of ring vibrations of C–O–C glycosidic band vibrations and C–OH side group stretching [34], indicating there is sugar in the form of pyranose [32]. There are α -type glycosidic bond types at 752 cm^{-1} and 911 cm^{-1} (Fig. 1A). The above results are consistent with those of Wang [26].

Table 1
Primers sequences of Real-time PCR.

Gene	Sequence (5'–3')	Sequence (3'–5')
<i>Sod1</i>	CGGATAAGAGAGGATGTT	TAGTACGGCCAATGATGGAATG
<i>Gpx3</i>	GACATCCGCTGGAACITTTGA	CCATCTTGACGTTGCTGACT
<i>Sod2</i>	AGCGTGACTTTGGGTCTTT	AGCGACCTTGCTCCTTATTG
<i>Gsta4</i>	GCTGGAGTGGAGITTTGAAGA	GTCAGTAGCATCCCGTCTATTT
<i>Cat</i>	CAGAGGAAAGCGGTCAAGAA	CATTCTTAGGCTTCTGGGAGTT
<i>Prdx3</i>	GGATTCCCACCTTCAGTCATCTT	AGTCTCGGGATATCTGCTTAGT
<i>Gsr</i>	ACCACGAGGAAGACGAAATG	ATCTCATCGCAGCCAATCC
<i>Mgst1</i>	CCACCTGAACGACCTTGAAA	CTGAAGTGAATGAGGGCTGTAG
<i>GAPDH</i>	GACATGCCCGCTGGAGAAAC	AGCCAGGATGCCCTTATG

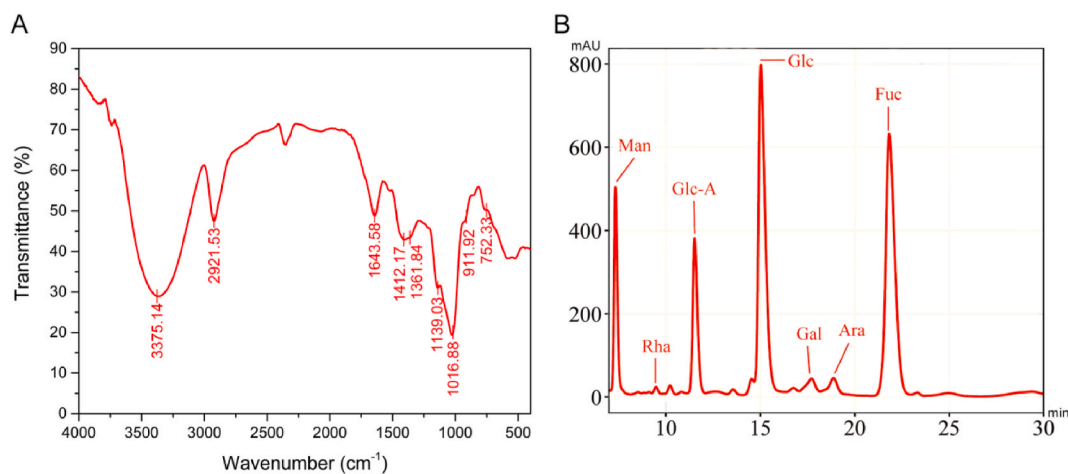


Fig. 1. Structural analysis spectrum of ILP. (A) FTIR spectrum of ILP; (B) HPLC spectrum of ILP.

3.2. Monosaccharide composition analysis of ILP

The results of the monosaccharide composition of the ILP detected by HPLC are shown in Fig. 1B. The composition and proportions of ILP are shown in Table 2. These results indicate that the main monosaccharide component of ILP consists of Man, Glc-A, Glc, and Fuc, and Fuc was the most abundant. Small amounts of Ara, Gal, and Rha were detected.

3.3. ILP treatment normalizes the estrous cycle of PCOS rats

The estrous cycle of rats was examined to establish the effectiveness of the PCOS model. Vaginal smears were performed and the cell morphology was observed by Papanicolaou staining to monitor the estrous cycle changes. Proestrus: mainly epithelial cells with a nucleus, and a few leukocytes and cornified cells; estrus: predominantly cornified cells with a few epithelial cells and leukocytes; metestrus: leukocytes, cornified cells, and nucleated epithelial cells were present; diestrus: mostly leukocytes (Fig. 2A). A disruption in the estrous cycle was observed in PCOS rats. In the PCOS group, rats spent a longer period in diestrus, but this disturbance was alleviated by ILP treatment (Fig. 2B).

3.4. Effect of ILP on body weight and ovarian weight in PCOS rats

The initial body weight of the groups did not differ significantly (Fig. 3A), but the PCOS rats put on weight rapidly during the modeling period (Fig. 3C). The PCOS rats' final body weighed 18.70% ($p < 0.05$) heavier than the normal rats (Fig. 3B), and the relative weight of the ovaries was 24.14% ($p < 0.05$) heavier than that of the normal group (Fig. 3D). ILP and Met reduced rats' body weight by 5.98% and 13.59%, respectively ($p < 0.05$). ILP also reduced the relative weight of the rat ovaries by 14.35% ($p < 0.05$); Met also decreased the relative weight of the rat ovaries, but not significantly.

3.5. ILP reverses histomorphological changes in PCOS rats ovaries

The pale color of ovaries was observed in the PCOS rats, while their size and weight also increased. And a pale uterus and insufficient blood supply were present. ILP effectively improved the blood supply to the ovaries and uterus (Fig. 4C). Light microscopic observation of the H&E staining revealed that normal rats had multiple corpus luteum and developing in different stages follicles. The PCOS rats showed polycystic-like changes in the ovaries, with an increased cystic follicle count and decreased corpus luteum (Fig. 4A). Furthermore, fibrosis was also found in the ovaries of PCOS rats according to Masson staining results. After treatment with Met and ILP, rats with PCOS experienced reduced ovarian fibrosis (Fig. 4B, D).

3.6. ILP treatment normalizes sex hormone levels in PCOS rats

Since letrozole is an aromatase inhibitor that raises androgens levels by inhibiting the activity of aromatase. The PCOS rats

Table 2
The monosaccharide composition of ILP.

Composition (%)	Gal	Glc	D-GlcA	Rha	Man	Ara	Fuc
ILP	1.67	23.19	9.83	2.93	6.89	1.61	53.15

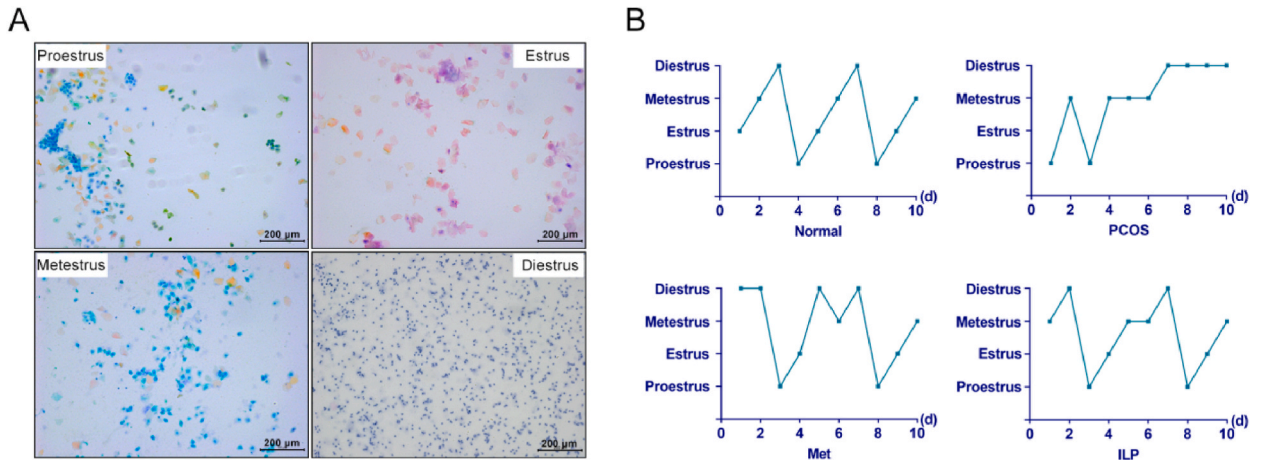


Fig. 2. Rats estrous cycle image. (A) Graph of Papanicolaou staining of cells (× 100). (B) Estrous cycle recording curves.

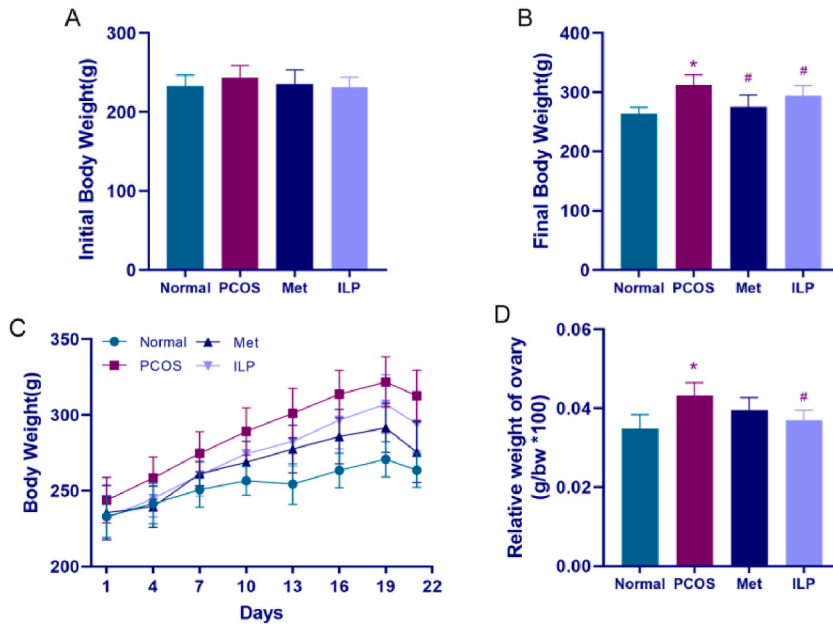


Fig. 3. Met and ILP effects on body weight and relative ovary weight. (A) Initial body weight; (B) final body weight; (C) body weight curves; (D) relative weight of ovary (n = 8). Versus the Normal group, **p* < 0.05 and ***p* < 0.01; versus the PCOS group, #*p* < 0.05 and ##*p* < 0.01. Statistics are the mean ± SD.

dramatically raised LH, LH/FSH and T levels by 23.55%, 31.02%, and 51.25% (*p* < 0.05), respectively, versus the normal rats (Fig. 5A, C, D). However, the E2 and FSH levels were markedly reduced by 23.14% and 34.64% (*p* < 0.05) (Fig. 5B, E). ILP significantly reduced the T levels by 21.44% and the LH levels by 18.66% (*p* < 0.05) and raised the E2 levels by 23.14% (*p* < 0.05). Met decreased the T and LH levels by 25.98% and 22.87% (*p* < 0.05), respectively, and raised the E2 levels by 21.52% (*p* < 0.05). Both ILP and Met had an insignificant effect on the FSH and LH/FSH levels.

3.7. ILP improves glucolipid metabolism levels in PCOS rats

PCOS patients may also have insulin resistance (IR), impaired glucose metabolism, dyslipidemia and abdominal obesity. The FBG and INS levels of PCOS rats were 12.09% and 29.87% more than the normal rats respectively (*p* < 0.05), and the HOMA-IR was similarly increased by 34.09% (*p* < 0.05) (Fig. 6A–C). With ILP and Met treatments, FBG levels declined by 11.62% and 17.47% (*p* < 0.05), INS levels by 17.47% and 19.37% (*p* < 0.05), and HOMA-IR by 20.15% and 19.77% (*p* < 0.05), respectively. LDL-C, TC and TG, which reflect the level of lipid metabolism, were also significantly elevated in the PCOS rat versus the normal rat by 50%, 44.68%, and

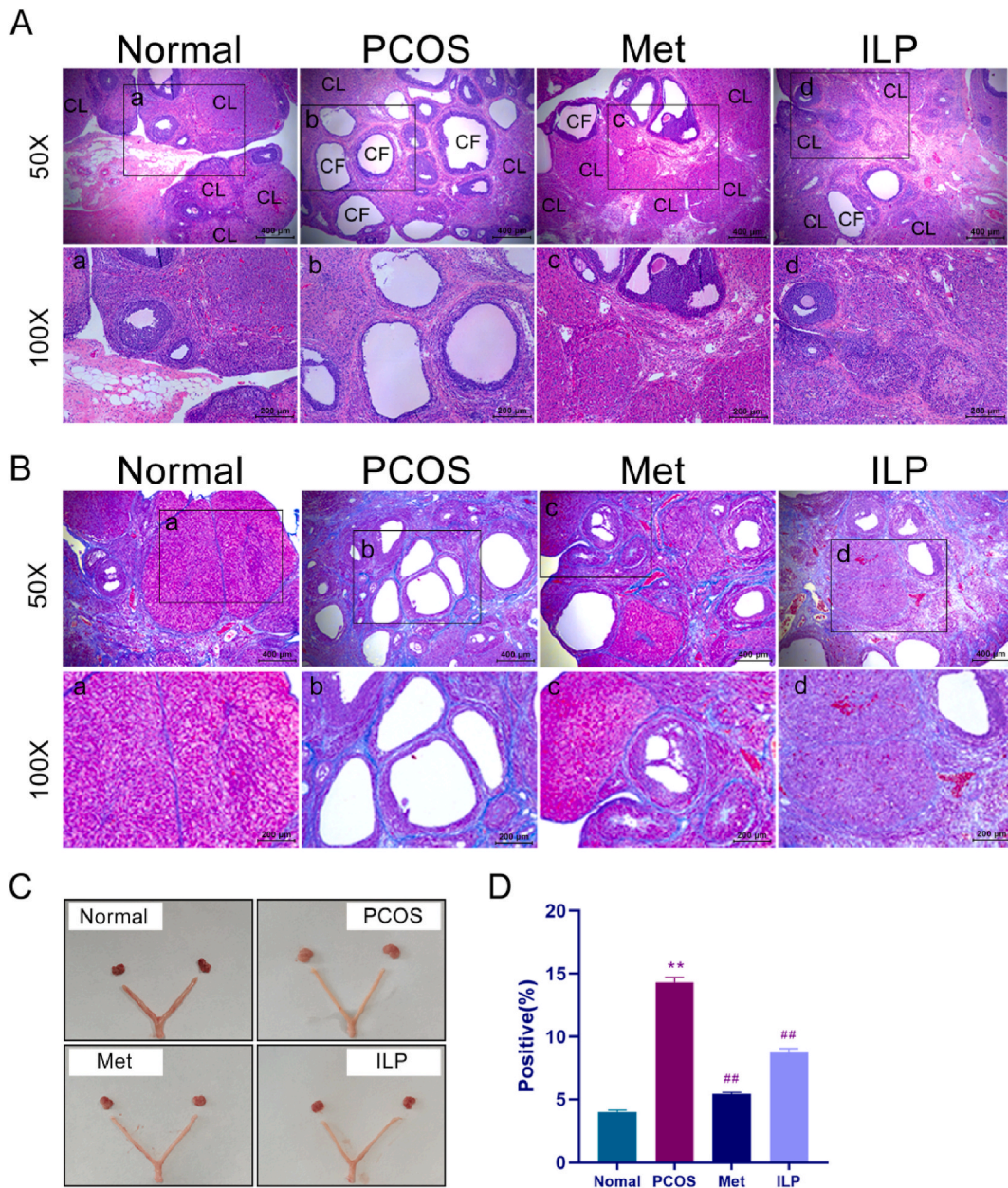


Fig. 4. Morphological effects of ovary and uterus and ovarian fibrosis. (A) Ovarian H&E staining (scale bar = 400 μm; the amplified area is defined by the black rectangle, high magnification scale bar = 200 μm), CL: corpus luteum, CF: cystic follicle; (B) Ovarian tissue stained with Masson (scale bar = 400 μm; the amplified area is defined by the black rectangle, high magnification scale bar = 200 μm); (C) Image of the uterus and ovaries; (D) positive of ovarian fibrosis.

1.82 times ($p < 0.05$), respectively. And the HDL-C levels were lessened by 39.24% ($p < 0.05$). The ILP and Met interventions both reduced TC levels by 17.84% ($p < 0.05$), TG levels by 23.53% and 16.18% ($p < 0.05$), and LDL-C levels by 42.99% and 30.84% ($p < 0.05$), respectively. At the same time, HDL-C levels increased by 29.17% and 47.92% ($p < 0.05$) (Fig. 7A–D). As determined by the H&E staining (Fig. 7E), PCOS rats have bigger peri-uterine adipocytes than ILP rats (Fig. 7F). All of the above indicates that ILP may be able to treat the problems of glucolipid metabolism in PCOS rats.

3.8. ILP reduces PCOS rat oxidative stress

OS affects PCOS etiology, contributing to IR, androgen excess, and chronic inflammation. There is a tendency for PCOS women to have abnormal OS biomarkers [35]. In our experiments, we measured rats’ serum levels of SOD and MDA. The SOD levels were

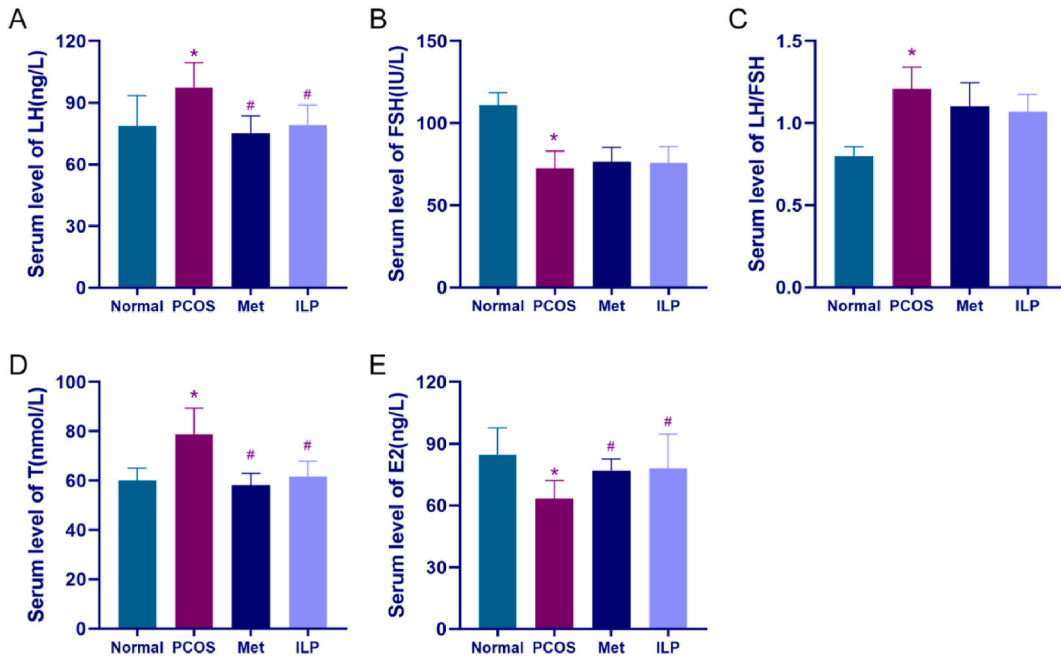


Fig. 5. The levels of (A) LH, (B) FSH, (C) LH/FSH, (D) T, and (E) E2 in the serum of rats (n = 8). Versus the Normal group, **p* < 0.05 and ***p* < 0.01; versus the PCOS group, #*p* < 0.05 and ##*p* < 0.01. Statistics are the mean ± SD.

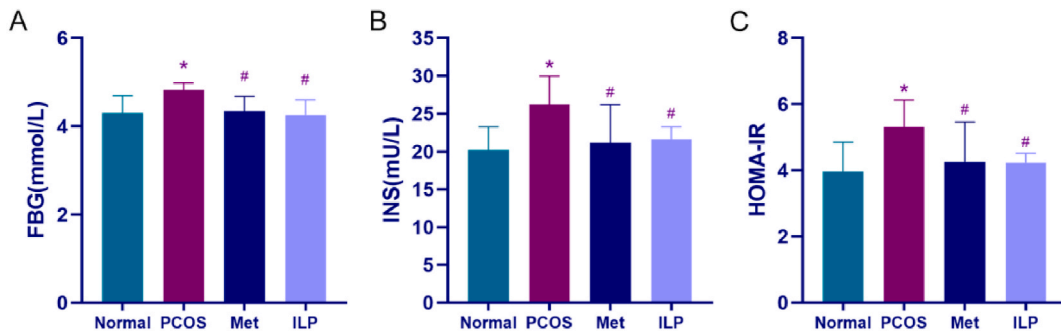


Fig. 6. (A) FBG, (B) INS, (C) and HOMA-IR levels of rats (n = 8). Versus the Normal group, **p* < 0.05 and ***p* < 0.01; versus the PCOS group, #*p* < 0.05 and ##*p* < 0.01. Statistics are the mean ± SD.

markedly lowered by 6.16% (*p* < 0.05) while MDA levels were raised by 78.32% (*p* < 0.01) in PCOS rats. ILP and Met increased SOD levels by 7.32% and 6.43% (*p* < 0.05) and decreased MDA levels by 32.16% and 37.65% (*p* < 0.01) in PCOS rats, respectively (Fig. 8A and B). For the purpose of further research on the impact on OS in PCOS of ILP, we also measured the levels of some antioxidant enzymes (*Sod1*, *Gpx3*, *Cat*, *Prdx3*, *Gsta4*, *Sod2*, *Mgst1* and *Gsr*) in ovarian tissues. The results showed that the levels of *Sod1*, *Gpx3*, *Sod2*, *Gsta4*, *Cat*, *Prdx3*, *Gsr* and *Mgst1* were dramatically decreased by 40%, 80%, 59%, 32%, 58%, 64%, 63% and 31% (*p* < 0.05) in PCOS group. The levels of *Sod1*, *Gpx3*, *Sod2*, *Gsta4*, *Cat*, *Prdx3*, *Gsr* and *Mgst1* were increased by 48.33%, 1.15 times, 1 time, 1.51 times, 1.90 times, 88.89%, 1.73 times and 89.86% (*p* < 0.05) in ILP group, respectively. The *Sod1*, *Gpx3*, *Sod2*, *Gsta4*, *Cat*, *Prdx3*, *Gsr* and *Mgst1* levels in the ovaries of Met group rats were elevated by 53.33%, 1.25 times, 80.49%, 53.62%, 1.43 times, 41.67%, 1.27 times and 53.62% (*p* < 0.01), respectively (Fig. 8C–J). Based on the above evidence, PCOS rats achieved a greater antioxidant capacity and experienced reduced OS with ILP and Met supplementation.

3.9. Affect of ILP on TGF-β1/smad pathway protein expression

PCOS patients often have interstitial ovarian fibrosis, which has been studied in association with an abnormal increase in TGF-β1 expression. In order to determine whether ILP has any effect on PCOS rats' ovarian fibrosis, we investigated the classical TGF-β1/Smad pathway. By analysis, the protein expression of *p-Smad2*, *p-smad3*, TGF-β1, TGF-βRI, and *Smad4* were higher than normal group by 48.99%, 33.26%, 1.54 times, 70.99%, and 63.03% (*p* < 0.01), respectively (Fig. 9A–F), while *smad7* expression adjusted downwards

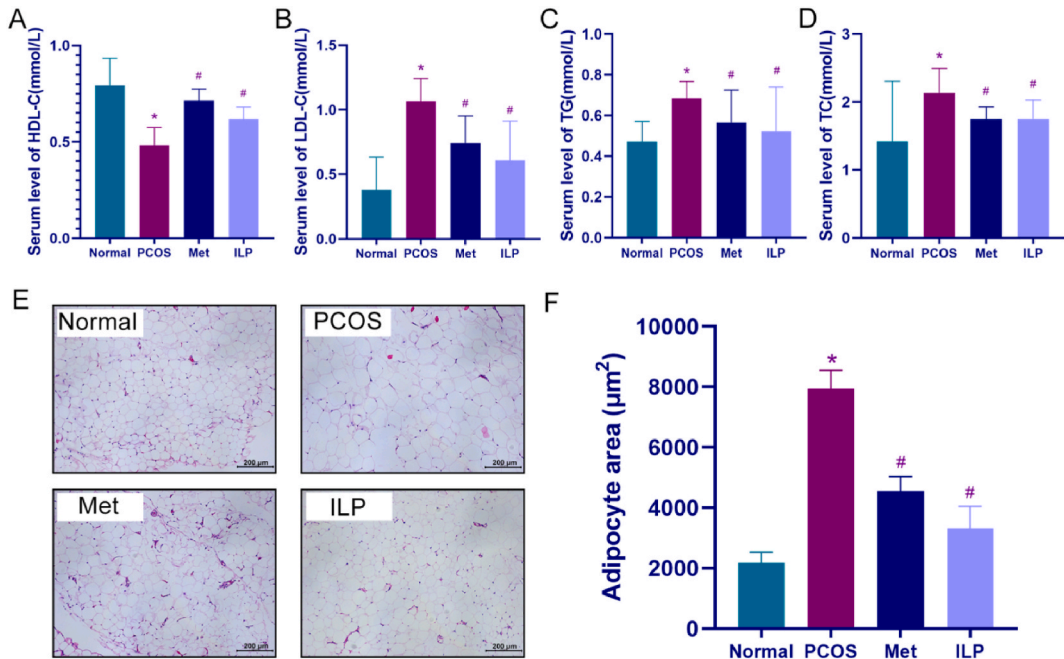


Fig. 7. (A) HDL-C, (B) LDL-C, (C) TG, (D) TC levels in the serum of rats, (E) image of periuterine adipocytes, (F) and adipocyte area of rats (n = 8). Versus the Normal group, *p < 0.05 and **p < 0.01; versus the PCOS group, #p < 0.05 and ##p < 0.01. Statistics are the mean ± SD.

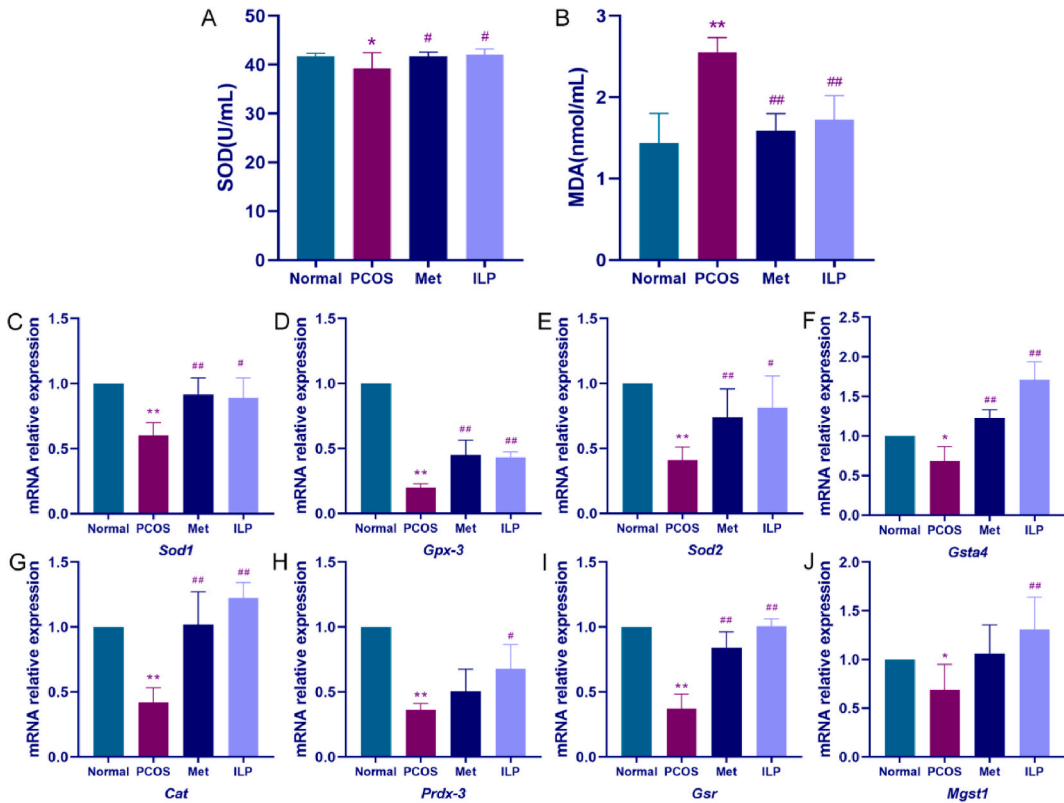


Fig. 8. The levels of (A) SOD, (B) MDA, (C) *Sod1*, (D) *Gpx-3*, (E) *Sod2*, (F) *Gsta4*, (G) *Cat*, (H) *Prdx-3*, (I) *Gsr*, (J) and *Mgst1* of rats (n = 8). Versus the Normal group, *p < 0.05 and **p < 0.01; versus the PCOS group, #p < 0.05 and ##p < 0.01. Statistics are the mean ± SD.

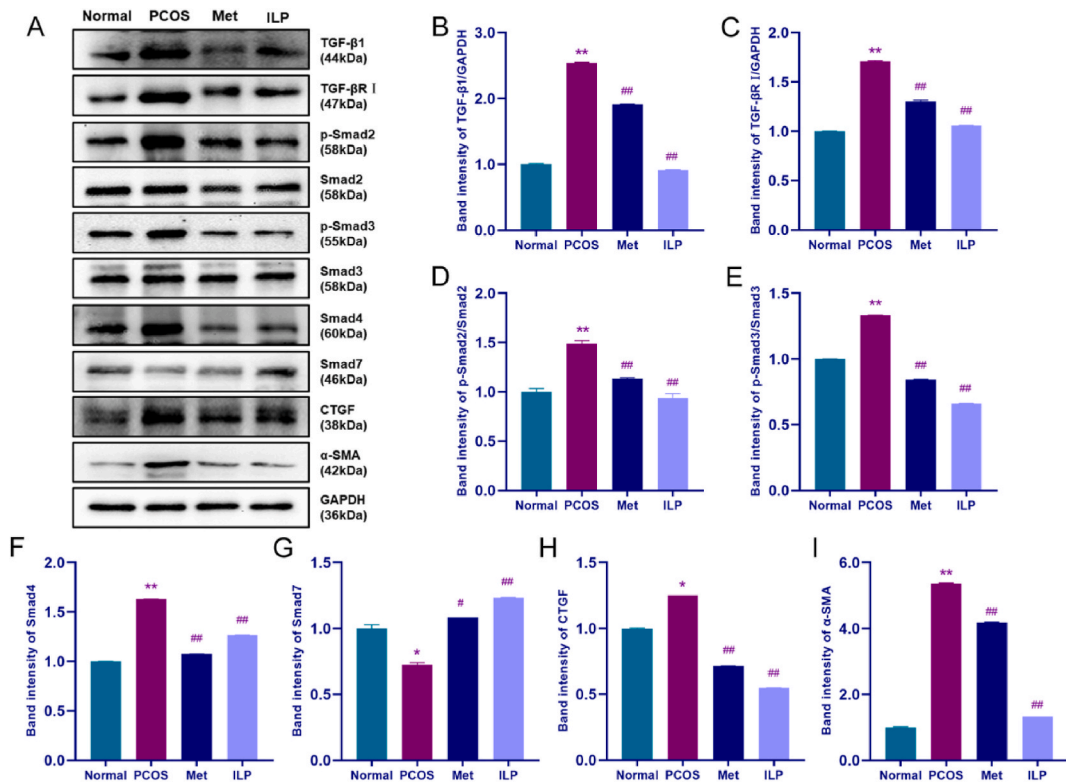


Fig. 9. Protein expressions in the rats' ovarian. Western blot of (A) TGF- β 1, TGF- β RI, p-Smad2, p-Smad3, Smad4, Smad7, CTGF, α -SMA, and GAPDH. Quantitative analysis of (B) TGF- β 1, (C) TGF- β RI, (D) p-Smad2, (E) p-Smad3, (F) Smad4, (G) Smad7, (H) CTGF, and (I) α -SMA in the ovary (n = 3). Versus the Normal group, * p < 0.05 and ** p < 0.01; versus the PCOS group, # p < 0.05 and ## p < 0.01. Statistics are the mean \pm SD.

by 27.38% (p < 0.05) (Fig. 9A, G). The expression of p-Smad2, p-Smad3, TGF- β 1, TGF- β RI, and Smad4 in the ILP and Met groups were less than PCOS group by 37.05% and 23.90% (p < 0.01), 50.51% and 36.63% (p < 0.01), 64.09% and 24.80% (p < 0.01), 38.10% and 23.60% (p < 0.01), and 22.26% and 33.96% (p < 0.01), respectively. The smad7 protein expression was upregulated by 69.84% (p < 0.01) and 49.15% (p < 0.05) in the Met and ILP rats, respectively, in comparison with the PCOS rats. Moreover, α -smooth muscle actin (α -SMA) and connective tissue growth factor (CTGF) expression in the ovaries of PCOS rats were also greatly more positive than normal rats by 4.37 times (p < 0.01) and 25.19% (p < 0.05), respectively. In the ILP and Met groups, CTGF and α -SMA expression levels were reduced by 56.32% and 75.27% (p < 0.01) and 42.88% and 22.03% (p < 0.01) respectively (Fig. 9A, H–I).

3.10. IHC staining for ILP treatment in rat ovarian fibrosis

Immunocytochemistry (IHC) staining of ovarian tissue sections showed the same results as the western blots. The area of positive expression of Smad4, Smad3, Smad2 and TGF- β 1 in PCOS rats was increased by 85.63%, 69.32%, 87.32% and 1.86 times, respectively (p < 0.01), comparison with the normal rats, while Smad7 was declined by 53.48% (p < 0.01) (Fig. 10A–J). Smad4, Smad3, Smad2, and TGF- β 1 positive expression areas in the ILP and Met groups decreased by 50.45% and 54.12% (p < 0.01), 55.79% and 48.03% (p < 0.01), 37.03% and 31.27% (p < 0.01), 52.04% and 54.16% (p < 0.01), whereas the Smad7 area elevated by 73.06% and 63.69% (p < 0.01), respectively.

4. Discussion

The imbalance of the hypothalamic-pituitary-ovarian axis (HPOA) is an important pathophysiological basis of PCOS. And in the development of PCOS, hyperactivity of GnRH neurons in the hypothalamus plays a critical role [36]. In PCOS patients, excessive androgens in the ovaries make the GnRH pulse generator insensitive to negative feedback inhibition, causing a sustained increase in pulse frequency, which increases LH excretion and restricts FSH excretion. An increased frequency of GnRH pulses promotes LH synthesis, contributing to the abnormal production of sex hormones and the dysfunction of the ovary [37]. High pulse release of LH causes follicular membrane cells to enhance the expression of the cytochrome P450c17 (CYP17), steroidogenic acute regulatory protein (STAR) and β -hydroxysteroid dehydrogenase (β -HSD), which increases the steroidogenic activity of follicular membrane cells, leading to androstenedione production [38]. Then, under the influence of FSH in the pituitary gland, the aromatase in granulosa cells converts androstenedione into estrogen. However, the relative lack of FSH secretion impairs and hinders follicular development,

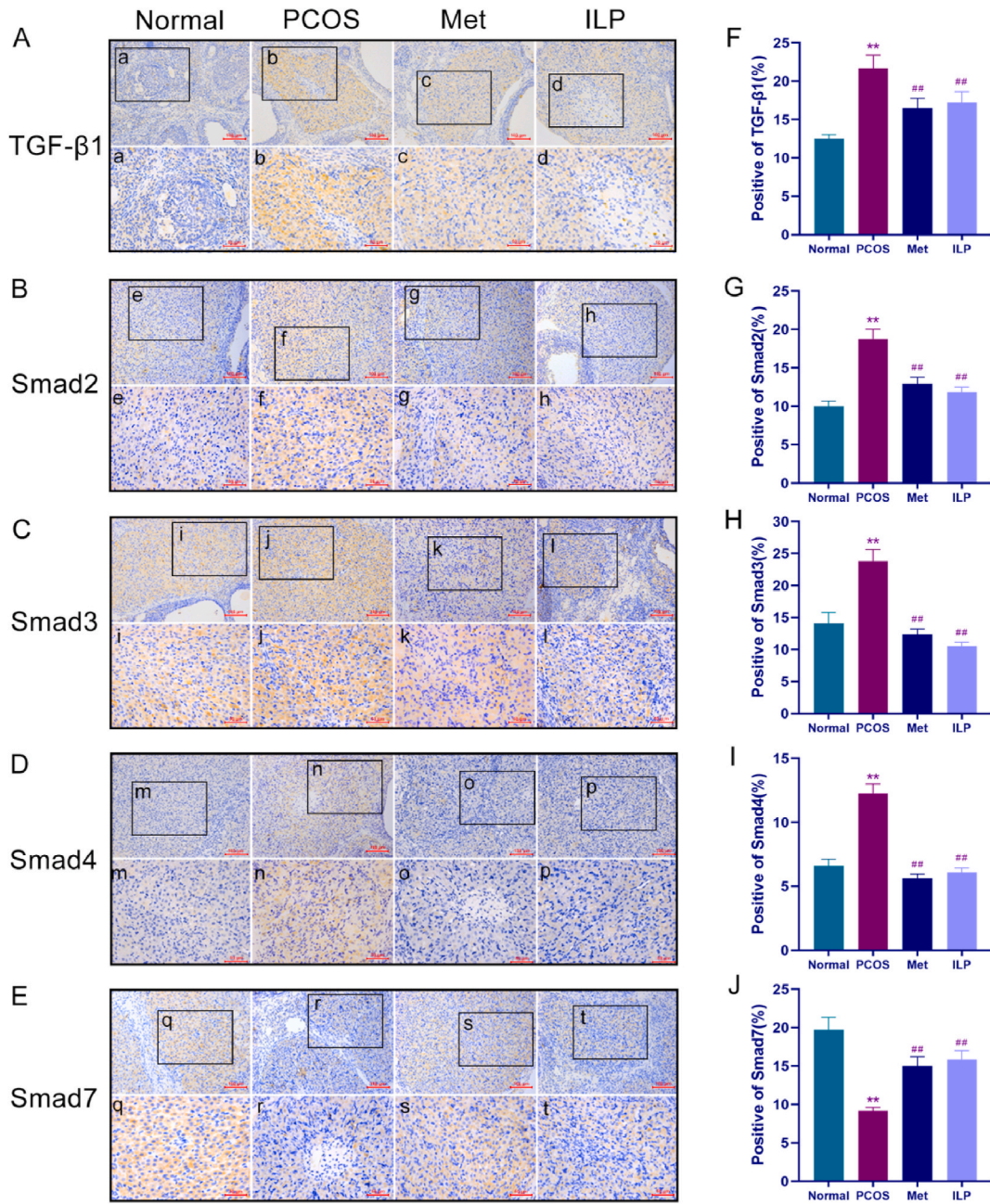


Fig. 10. Area of positive TGF-β1, Smad2, Smad3, Smad4, and Smad7 expression in the rats ovaries. The figures illustrate the immunohistochemistry profiles of (A) TGF-β1, (B) Smad2, (C) Smad3, (D) Smad4, (E) and Smad7 proteins in the ovary. (scale bar = 100 μm; the amplified area is defined by the black rectangle, high magnification scale bar = 50 μm). The positive of (F) TGF-β1, (G) Smad2, (H) Smad3, (I) Smad4, (J) and Smad7 in the ovary (n = 3). Versus the Normal group, *p < 0.05 and **p < 0.01; versus the PCOS group, #p < 0.05 and ##p < 0.01. Statistics are the mean ± SD.

leading to hyperandrogenemia among PCOS women [39]. In our experiments, we found that PCOS rats had abnormal levels of sex hormones. The LH, T and LH/FSH levels were raised, and FSH and E2 levels were declined in PCOS rats. This is because the letrozole used in our modeling is an aromatase inhibitor. Aromatase is the final rate-limiting enzyme in the transformation from androgens to estrogens. A decline in its activity can cause a hyperandrogenic environment in the body, which leads to elevated levels of T in PCOS rats [40]. There is increasing evidence that high levels of T may lead to an abnormal frequency of GnRH release, resulting in more LH production by the hypophysis [41], thus increasing the LH/FSH [42]. LH/FSH is an important marker for assessing the function of the ovaries and aiding in the diagnosis of PCOS [43]. A rise in LH/FSH ratio is more often due to the development of LH levels rather than a decline in the levels of FSH [44]. In addition, GnRH also affects the secretion of FSH, which stimulates follicular growth and E2

synthesis [45]. The increased frequency of GnRH stimulation favors LH production to the detriment of FSH [46]. This explains the elevation of T caused by letrozole inhibiting the transformation of androgens into estrogens in our experiments. This contributes to an abnormally high frequency of GnRH pulses, which drives more LH secretion and inhibits FSH synthesis. Moreover, it also prevents normal follicle growth and reduces E2 synthesis, which ultimately leads to ovulation disorders. In our study, ILP and Met normalized the sex hormone levels, reduced LH and T secretion, and decreased the LH/FSH in PCOS rats. They also promoted the FSH and E2 synthesis (Fig. 5A–E), contributing to follicles in different developmental stages with multiple corpus luteum while restoring the histological morphology of the ovary (Fig. 4A).

Previous studies have also revealed that androgen excess is often strongly associated with metabolic disorders, especially for PCOS [47]. Chronic androgen excess may cause patients with PCOS to develop abdominal obesity. Abdominal obesity is related to impaired androgen homeostasis and the overactivity of the hypothalamic-pituitary-adrenal (HPA) axis [48]. In the initial phase, the initial body weight of the groups did not differ significantly. The PCOS rats gained weight significantly, both ILP and Met were effective in slowing down their rate of weight gain (Fig. 3A, B, D). In this study, the significant weight gain in PCOS rats was related to their abnormally elevated levels of T. In addition, their increase in relative ovarian weight was due to ovarian lipid accumulation and follicular fluid accumulation in cystic follicles [49] (Fig. 3C). The LDL-C, TC, and TG levels were raised, while the HDL-C levels were lessened in PCOS rats. Both ILP and Met treatments improved these parameters, and it can be seen that ILP had a superior treatment effect compared to Met (Fig. 7A–D). It was further observed that PCOS rats had a larger adipocyte area, which was reduced after treatment with ILP and Met (Fig. 7E). There is increasing evidence that excessive androgen secretion can contribute to adipogenesis and that lipid metabolism is disturbed in PCOS, contributing to obesity. The above results indicate that ILP can effectively inhibit fat formation and it has good lipid-lowering potential.

Furthermore, androgen excess is often related to IR in obese women, especially those with PCOS [50]. Excess androgens have a positive correlation between HOMA-IR and insulin levels [51,52]. It is common for PCOS patients to experience IR, leading to an overproduction of androgens, which reduces the release of sex hormone-binding globulin (SHBG) [53]. Insulin is a crucial hormone involved in glucose metabolism, and its sensitivity is closely related to the normal uptake and metabolism of glucose [54]. IR is regarded as a deficiency in regulating glucose metabolism in tissues mediated by insulin (mainly liver, fat and muscle). Recent research has revealed that adipose tissue contributes to developing IR, possibly through the delivery of lipids and other circulating factors that promote IR [55]. This evidence suggests that both androgens and obesity are tightly linked to IR, and our study confirms this. PCOS rats had higher FBG and INS because IR makes insulin less efficient in promoting glucose uptake and utilization, and the body compensates by secreting too much insulin. Their HOMA-IR values, an index for assessing IR levels, were also significantly higher (Fig. 6A–C), which may be caused by weight gain in PCOS rats. There was a marked downward trend in FBG, INS, and HOMA-IR levels with ILP and Met, and we infer that the reduced T levels in the above two treatment groups of rats may be related to the improvement of IR.

A further feature of PCOS is an increase in OS, such as intracellular reactive oxygen species (ROS), which is an essential pathway contributing to the disease's onset and progression [56]. Metabolic disturbances in PCOS produce more free radicals, leading to OS [57]. OS is the result of ROS and antioxidants are out of balance [58,59]. Some features of PCOS, such as an excess of androgens, IR, and obesity, may promote the progress of OS [60]. Adipose tissue expansion, such as obesity, is caused by adipocyte hypertrophy and subsequent hypoxic conditions that lead to OS and increased autophagy [61]. The abnormal metabolism of PCOS is partly because of the reaction of free radicals with lipids and peroxides generated during mitochondrial oxidation to produce MDA [62]. MDA is a lipid peroxidation product, it reflects the degree of oxidative damage in the body. SOD is a major antioxidant enzyme that has a significant impact on retaining the dynamic balance of oxidation-antioxidation and its level is an indicator of antioxidant capacity. Wang [25] demonstrated that ILP increased liver SOD levels and reduced MDA levels, indicating that it has some antioxidant activity. The study revealed that SOD levels were obviously lower in the serum of PCOS rats, while MDA levels presented much higher than normal (Fig. 8A and B). This indicates rats with PCOS exhibit an increased level of OS. As mentioned earlier, PCOS rats were heavier and had a larger adipocyte area, which is also due to the more severe OS. The above results showed that ILP was able to reduce the damage caused by OS in PCOS rats. To further investigate the antioxidant capacity of ILP, we examined the levels of some antioxidant enzymes (*Sod1*, *Gpx3*, *Gsta4*, *Sod2*, *Cat*, *Prdx3*, *Mgst1* and *Gsr*) in rat ovaries. According to this study, ILP was found to enhance these antioxidant enzyme expressions (Fig. 8C–J). These results indicate that ILP has a good antioxidant capacity and can ameliorate OS in PCOS rats.

There has been evidence in recent research that ovarian fibrosis has been observed in rats with androgen-induced PCOS, which may impair ovarian function [63]. The overproduction of androgens may disrupt the balance of matrix metalloproteinases-9 (MMP-9), MMP-2, and tissue inhibitors of metalloproteinase-1 (TIMP-1), TIMP-2 in the ovary, resulting in ovarian fibrosis in PCOS women [9]. According to research, obesity and IR are significantly and positively associated with cystic follicles, ovarian function, OS, and fibrosis [64]. In this experiment, Masson's staining revealed a notable growth in the percentage of collagen fiber area in PCOS rats' ovaries, indicating a higher deposition of fibrous tissue (Fig. 4B, D). Ovarian fibrosis may be due to the granulosa cells degenerate which leads to the proliferation of mesenchymal fibroblasts as well as the deposition of fibrin and collagen. Abnormal expression of ECM, CTGF, and profibrotic proteins TGF- β 1 may be a contributor to fibrosis [65]. A downstream mediator like Smad2 and Smad3 is revitalized by TGF- β 1 to exert its biological effects, while Smad7 exerts a negative regulatory effect on the pathways activated by TGF- β 1. TGF- β 1 interacts with TGF- β RII to activate TGF- β RI and then it phosphoric Smad2/Smad3, which generates a trimeric complex with Smad4 [66,67]. Subsequently, TGF- β 1/Smad complex may promote CTGF and α -SMA, transcription in the nucleus [63]. According to prior research, the TGF- β 1/Smad mechanism is a critical part of the pathogenesis in organ fibrosis [68–70]. Fig. 9A–G illustrates the manifestation in PCOS rat ovaries of TGF- β 1, TGF- β RI, p-Smad2/Smad2, p-Smad3/Smad3, and Smad4 were increased clearly, and the Smad7 expression level was noticeably reduced, compared to normal rats. This revealed the TGF- β 1/Smad is activated and involved in the development of fibrosis. According to IHC, there was more substantial growth than normal rats in the area of positive TGF- β 1, Smad2, Smad3, and Smad4 in ovarian sections from PCOS rats, while the area of positive Smad7 noticeably declined (Fig. 10A–J).

CTGF is a downstream factor induced by TGF- β 1. It is involved in mediating some of the profibrotic effects of TGF- β 1, such as increasing the synthesis and accumulation of ECM [71]. TGF- β 1 enhances the ability of lymphocytes, neutrophils, and monocytes to secrete CTGF. CTGF, which is induced by TGF- β 1, acts paracrine on mesenchymal fibroblasts, thereby stimulating the production of TGF- β 1 [63]. These two factors interact with each other to accelerate the development of fibrosis. A marker of myofibroblasts, α -SMA is a critical part of the development of fibrosis and has been considered a marker of tissue fibrogenic activity [72]. Meanwhile, the activation of CTGF and α -SMA was also observed in our experiments (Fig. 9A, H, I). ILP and Met both inhibited the induction of the TGF- β 1/Smad path and attenuated ovarian tissue fibrosis.

5. Conclusion

Overall, we found that ILP improved the histological changes, sex hormone homeostasis, disorders of glucolipid metabolism, and OS in PCOS rats. It reversed the symptoms of PCOS by modulating TGF- β 1/Smad pathway to ameliorate the fibrosis in rats' ovaries. These findings could serve as a foundation for clinical studies of ILP for treating PCOS, that is, ILP may provide an alternative treatment to PCOS by acting as an antioxidant. If the combination of ILP and metformin might show a better therapeutic effect, the interaction between the combination of Chinese and Western drugs deserves further consideration.

Author contribution statement

Yan-Yuan Zhou: Conceived and designed the experiments; Wrote the paper.

Ya-Qi Wu: Performed the experiments; Analyzed and interpreted the data; Wrote the paper.

Chao-Jie Chong: Performed the experiments; Analyzed and interpreted the data.

Shu-Mei Zhong; Zi-Xian Wang; Xiao-Hui Qin; Zhi-Qiang Liu; Jun-Yang Liu: Performed the experiments.

Jia-Le Song: Conceived and designed the experiments; Contributed reagents, materials, analysis tools or data.

Data availability statement

Data will be made available on request.

Funding

The authors gratefully acknowledge the financial support by the National Natural Science Foundation of China (81560530, 81760589, 81860767, 81960590, 82273630), the Special Funds for Guiding Local Scientific and Technological Development by the Central Government (Guike ZY22096025), the Guangxi Natural Science Foundation of China (2020GXNSFAA159160, 2022GXNSFAA035603), the Foundation for University Key Teachers by the Department of Education of Guangxi Zhuang Autonomous Region (Guirengjiao[2018]18), the Funding Scheme for High-level Overseas Chinese Students' Return of Ministry of Human Resources and Social Security (Renshetinghan[2019]160), Guangxi Medical and Health Key Cultivation Discipline Construction Project (Guiweikejiaofa[2022]4) and the Start-up Fund for the introduction of talents and scientific research of Guilin Medical University (04010150001).

Declaration of competing interest

The authors declare that they have no known competing financial interests or personal relationships that could have appeared to influence the work reported in this paper.

Appendix A. Supplementary data

Supplementary data to this article can be found online at <https://doi.org/10.1016/j.heliyon.2023.e18741>.

References

- [1] M.O. Goodarzi, D.A. Dumesic, G. Chazenbalk, R. Azziz, Polycystic ovary syndrome: etiology, pathogenesis and diagnosis, *Nat. Rev. Endocrinol.* 4 (2011) 219–231, [10.1038/nrendo.2010.217](https://doi.org/10.1038/nrendo.2010.217).
- [2] H. Shan, R. Luo, X. Guo, R. Li, Z. Ye, T. Peng, F. Liu, Z. Yang, Abnormal endometrial receptivity and oxidative stress in polycystic ovary syndrome, *Front. Pharmacol.* (2022), 904942, [10.3389/fphar.2022.904942](https://doi.org/10.3389/fphar.2022.904942).
- [3] M. Shokoohi, S.-H. Abtahi-Eivary, M. Moghimian, M. Soltani, H. Shoorei, H. Hajizadeh, The effect of galega officinalis on hormonal and metabolic profile in A rat model of polycystic ovary syndrome (PCOS), *International Journal of Women's Health and Reproduction Sciences* 6 (2018) 276–282, <https://doi.org/10.15296/ijwhr.2018.46>.
- [4] Y.L. Yang, W.W. Zhou, S. Wu, W.L. Tang, Z.W. Wang, Z.Y. Zhou, Z.W. Li, Q.F. Huang, Y. He, H.W. Zhou, Intestinal flora is a Key factor in insulin resistance and contributes to the development of polycystic ovary syndrome, *Endocrinology* 10 (2021), [10.1210/endo/bqab118](https://doi.org/10.1210/endo/bqab118).

- [5] F. Khodaeifar, S. Fazljou, A. Khaki, M. Torbati, E. Madarek, A. Khaki, M. Shokoohi, A. Dalili, Investigation the role of hydroalcoholic extract of *Apium graveolens* and cinnamon zeylanicum on metabolically change and ovarian oxidative injury in a rat model of PCOS, *International Journal of Women's Health and Reproduction Sciences* 7 (2018) 92–98, <https://doi.org/10.15296/ijwhr.2019.15>.
- [6] K.A. Walters, R.B. Gilchrist, W.L. Ledger, H.J. Teede, D.J. Handelsman, R.E. Campbell, New perspectives on the pathogenesis of PCOS: neuroendocrine origins, *Trends Endocrinol. Metabol.* 12 (2018) 841–852, [10.1016/j.tem.2018.08.005](https://doi.org/10.1016/j.tem.2018.08.005).
- [7] F. Wang, Z.F. Zhang, Y.R. He, H.Y. Wu, S.S. Wei, Effects of dipeptidyl peptidase-4 inhibitors on transforming growth factor- β 1 signal transduction pathways in the ovarian fibrosis of polycystic ovary syndrome rats, *J. Obstet. Gynaecol. Res.* 3 (2019) 600–608, [10.1111/jog.13847](https://doi.org/10.1111/jog.13847).
- [8] A. Garg, B. Patel, A. Abbara, W.S. Dhillon, Treatments targeting neuroendocrine dysfunction in polycystic ovary syndrome (PCOS), *Clin. Endocrinol.* 2 (2022) 156–164, [10.1111/cen.14704](https://doi.org/10.1111/cen.14704).
- [9] F. Zhou, L.B. Shi, S.Y. Zhang, Ovarian fibrosis: a phenomenon of concern, *Chin. Med. J. (Engl.)* 3 (2017) 365–371, [10.4103/0366-6999.198931](https://doi.org/10.4103/0366-6999.198931).
- [10] F. Verrecchia, A. Mauviel, Transforming growth factor-beta and fibrosis, *World J. Gastroenterol.* 22 (2007) 3056–3062, [10.3748/wjg.v13.i22.3056](https://doi.org/10.3748/wjg.v13.i22.3056).
- [11] H.H. Hu, D.Q. Chen, Y.N. Wang, Y.L. Feng, G. Cao, N.D. Vaziri, Y.Y. Zhao, New insights into TGF- β /Smad signaling in tissue fibrosis, *Chem. Biol. Interact.* (2018) 76–83, <https://doi.org/10.1016/j.cbi.2018.07.008>.
- [12] X. Chen, C. Tao, J. Wang, B. He, J. Xu, Meta-analysis of therapeutic efficacy and effects of integrated traditional Chinese and Western medicine on coagulation and fibrinolysis system in patients with threatened abortion and polycystic ovary syndrome, *Am. J. Transl. Res.* 5 (2022) 2768–2778.
- [13] R.S. Legro, H.X. Barnhart, W.D. Schlaff, B.R. Carr, M.P. Diamond, S.A. Carson, M.P. Steinkampf, C. Coutifaris, P.G. McGovern, N.A. Cataldo, G.G. Gosman, J. E. Nestler, L.C. Giudice, P.C. Leppert, E.R. Myers, Clomiphene, metformin, or both for infertility in the polycystic ovary syndrome, *N. Engl. J. Med.* 6 (2007) 551–566, [10.1056/NEJMoa063971](https://doi.org/10.1056/NEJMoa063971).
- [14] R.S. Legro, R.J. Zaino, L.M. Demers, A.R. Kunselman, C.L. Gnatuk, N.I. Williams, W.C. Dodson, The effects of metformin and rosiglitazone, alone and in combination, on the ovary and endometrium in polycystic ovary syndrome, *Am. J. Obstet. Gynecol.* 4 (2007), <https://doi.org/10.1016/j.ajog.2006.12.025>, 402 e401–410; discussion 402 e410–401.
- [15] C.Y. Kwon, I.H. Cho, K.S. Park, Therapeutic effects and mechanisms of herbal medicines for treating polycystic ovary syndrome: a review, *Front. Pharmacol.* (2020) 1192, [10.3389/fphar.2020.01192](https://doi.org/10.3389/fphar.2020.01192).
- [16] A. Mihanfar, M. Nouri, L. Roshangar, M.H. Khadem-Ansari, Ameliorative effects of fisetin in letrozole-induced rat model of polycystic ovary syndrome, *J. Steroid Biochem. Mol. Biol.* (2021), 105954, [10.1016/j.jsbmb.2021.105954](https://doi.org/10.1016/j.jsbmb.2021.105954).
- [17] A. Manouchehri, S. Abbaszadeh, M. Ahmadi, F.K. Nejad, M. Bahmani, N. Dastyar, Polycystic ovaries and herbal remedies: a systematic review, *J. Bras. Reprod. Assist.* 27 (2022) 85–91, <https://doi.org/10.5935/1518-0557.20220024>.
- [18] X. Feng, D. Wang, L. Hu, H. Lu, B. Ling, Y. Huang, Q. Jiang, Dendrobium officinale polysaccharide ameliorates polycystic ovary syndrome via regulating butyrate dependent gut-brain-ovary axis mechanism, *Front. Endocrinol.* (2022), 962775, [10.3389/fendo.2022.962775](https://doi.org/10.3389/fendo.2022.962775).
- [19] M. Rondanelli, A. Riva, G. Petrangolini, P. Allegrini, A. Giacosa, T. Fazia, L. Bernardinelli, C. Gasparri, G. Peroni, S. Perna, Berberine phospholipid is an effective insulin sensitizer and improves metabolic and hormonal disorders in women with polycystic ovary syndrome: a one-group pretest-post-test explanatory study, *Nutrients* 10 (2021), 10.3390/nu13103665.
- [20] W. Li, H. Hu, G. Zou, Z. Ma, J. Liu, F. Li, Therapeutic effects of puerarin on polycystic ovary syndrome: a randomized trial in Chinese women, *Medicine* 21 (2021), e26049, [10.1097/md.00000000000026049](https://doi.org/10.1097/md.00000000000026049).
- [21] R.M. Chugh, P. Mittal, N. Mp, T. Arora, T. Bhattacharya, H. Chopra, S. Cavalu, R.K. Gautam, Fungal mushrooms: a natural compound with therapeutic applications, *Front. Pharmacol.* (2022), 925387, [10.3389/fphar.2022.925387](https://doi.org/10.3389/fphar.2022.925387).
- [22] Y. Zhang, G. Zhang, J. Ling, Medicinal fungi with antiviral effect, *Molecules* 14 (2022), 10.3390/molecules27144457.
- [23] Y. Yu, M. Shen, Q. Song, J. Xie, Biological Activities and Pharmaceutical Applications of Polysaccharide from Natural Resources: A Review, *Carbohydrate Polymers*, 2018, pp. 91–101, [10.1016/j.carbpol.2017.12.009](https://doi.org/10.1016/j.carbpol.2017.12.009).
- [24] L. Sun, X. Li, H. Ma, R. He, P.O. Donkor, Global gene expression changes reflecting pleiotropic effects of *Irpex lacteus* induced by low-intensity electromagnetic field, *Bioelectromagnetics* 2 (2019) 104–117, [10.1002/bem.22171](https://doi.org/10.1002/bem.22171).
- [25] J. Wang, C. Li, W. Hu, L. Li, G. Cai, Y. Liu, D. Wang, Studies on the anti-fatigue activities of *Irpex lacteus* polysaccharide-enriched extract in mouse model, *Pak. J. Pharm. Sci.* 3 (2019) 1011–1018.
- [26] J. Wang, J. Song, D. Wang, N. Zhang, J. Lu, Q. Meng, Y. Zhou, N. Wang, Y. Liu, D. Wang, L. Teng, The anti-membranous glomerulonephritic activity of purified polysaccharides from *Irpex lacteus* Fr, *Int. J. Biol. Macromol.* (2016) 87–93, [10.1016/j.ijbiomac.2015.11.087](https://doi.org/10.1016/j.ijbiomac.2015.11.087).
- [27] X. Meng, C. Che, J. Zhang, Z. Gong, M. Si, G. Yang, L. Cao, J. Liu, Structural characterization and immunomodulating activities of polysaccharides from a newly collected wild *Morchella sextelata*, *Int. J. Biol. Macromol.* (2019) 608–614, [10.1016/j.ijbiomac.2019.01.226](https://doi.org/10.1016/j.ijbiomac.2019.01.226).
- [28] Y. Zhou, H. Lan, Z. Dong, W. Li, B. Qian, Z. Zeng, W. He, J.L. Song, Rhamnocitrin attenuates ovarian fibrosis in rats with letrozole-induced experimental polycystic ovary syndrome, *Oxid. Med. Cell. Longev.* (2022), 5558599, [10.1155/2022/5558599](https://doi.org/10.1155/2022/5558599).
- [29] Y. Zhou, H. Lan, Z. Dong, W. Cao, Z. Zeng, J.L. Song, Dietary proanthocyanidins alleviated ovarian fibrosis in letrozole-induced polycystic ovary syndrome in rats, *J. Food Biochem.* 5 (2021), e13723, [10.1111/jfbc.13723](https://doi.org/10.1111/jfbc.13723).
- [30] K.F. Hua, M.Y. Zhang, Y. Zhang, B.J. Ren, Y.H. Wu, Characteristics of OGTT and correlation between the insulin to C-peptide molar ratio, HOMA-IR, and insulin antibodies in T2DM patients, *Diabetes Metab. Syndr. Obes.* (2022) 2417–2425, [10.2147/dmso.S373475](https://doi.org/10.2147/dmso.S373475).
- [31] N. Peker, U. Değer, F. Asir, Investigation of the effects of carvedilol on experimental ischemia/reperfusion model of rat ovaries by immunohistochemistry, *Anal. quant. cytopathol.* (2020) 197–204.
- [32] X. Yang, M. Huang, C. Qin, B. Lv, Q. Mao, Z. Liu, Structural characterization and evaluation of the antioxidant activities of polysaccharides extracted from Qingzhuang brick tea, *Int. J. Biol. Macromol.* (2017) 768–775, [10.1016/j.ijbiomac.2017.03.189](https://doi.org/10.1016/j.ijbiomac.2017.03.189).
- [33] B. Souza, M.A. Cerqueira, A.I. Bourbon, A.C. Pinheiro, J.T. Martins, J.A. Teixeira, M.A. Coimbra, A.A.J.F.H. Vicente, Chemical characterization and antioxidant activity of sulfated polysaccharide from the red seaweed *Gracilaria birdiae*, *Food Hydrocolloids* 2 (2012) 287–292, [10.1016/j.foodhyd.2011.10.005](https://doi.org/10.1016/j.foodhyd.2011.10.005).
- [34] Y. Wu, S.W. Cui, J. Tang, Q. Wang, X. Gu, Preparation, partial characterization and bioactivity of water-soluble polysaccharides from boat-fruited *sterculia* seeds, *Carbohydr. Polym.* 4 (2007) 437–443, [10.1016/j.carbpol.2007.05.010](https://doi.org/10.1016/j.carbpol.2007.05.010).
- [35] P. Dubey, S. Reddy, S. Boyd, C. Bracamontes, S. Sanchez, M. Chattopadhyay, A. Dwivedi, Effect of nutritional supplementation on oxidative stress and hormonal and lipid profiles in PCOS-affected females, *Nutrients* 9 (2021), 10.3390/nu13092938.
- [36] B. Liao, J. Qiao, Y. Pang, Central regulation of PCOS: abnormal neuronal-reproductive-metabolic circuits in PCOS pathophysiology, *Front. Endocrinol.* (2021), 667422, [10.3389/fendo.2021.667422](https://doi.org/10.3389/fendo.2021.667422).
- [37] C.R. McCartney, R.E. Campbell, J.C. Marshall, S.M. Moenter, The role of gonadotropin-releasing hormone neurons in polycystic ovary syndrome, *J. Neuroendocrinol.* 5 (2022), e13093, [10.1111/jne.13093](https://doi.org/10.1111/jne.13093).
- [38] E. Diamanti-Kandaraki, G. Argyrakopoulou, F. Economou, E. Kandaraki, M. Koutsilieris, Defects in insulin signaling pathways in ovarian steroidogenesis and other tissues in polycystic ovary syndrome (PCOS), *J. Steroid Biochem. Mol. Biol.* 3–5 (2008) 242–246, [10.1016/j.jsbmb.2008.03.014](https://doi.org/10.1016/j.jsbmb.2008.03.014).
- [39] R. Dadachanji, N. Shaikh, S. Mukherjee, Genetic variants associated with hyperandrogenemia in PCOS pathophysiology, *Genet. Res. Int.* (2018), 7624932, [10.1155/2018/7624932](https://doi.org/10.1155/2018/7624932).
- [40] S. Patel, Disruption of aromatase homeostasis as the cause of a multiplicity of ailments: a comprehensive review, *J. Steroid Biochem. Mol. Biol.* (2017) 19–25, [10.1016/j.jsbmb.2017.01.009](https://doi.org/10.1016/j.jsbmb.2017.01.009).
- [41] D. De Ziegler, K. Steingold, M. Cedars, J.K. Lu, D.R. Meldrum, H.L. Judd, R.J. Chang, Recovery of hormone secretion after chronic gonadotropin-releasing hormone agonist administration in women with polycystic ovarian disease, *J. Clin. Endocrinol. Metab.* 6 (1989) 1111–1117, [10.1210/jcem-68-6-1111](https://doi.org/10.1210/jcem-68-6-1111).
- [42] V. De Leo, A. la Marca, F. Petraglia, Insulin-lowering agents in the management of polycystic ovary syndrome, *Endocr. Rev.* 5 (2003) 633–667, [10.1210/er.2002-0015](https://doi.org/10.1210/er.2002-0015).
- [43] M.T. Le, V.N.S. Le, D.D. Le, V.Q.H. Nguyen, C. Chen, N.T. Cao, Exploration of the role of anti-Mullerian hormone and LH/FSH ratio in diagnosis of polycystic ovary syndrome, *Clin. Endocrinol.* 4 (2019) 579–585, [10.1111/cen.13934](https://doi.org/10.1111/cen.13934).

- [44] R.B. Barnes, R.L. Rosenfield, S. Burstein, D.A. Ehrmann, Pituitary-ovarian responses to nafarelin testing in the polycystic ovary syndrome, *N. Engl. J. Med.* 9 (1989) 559–565, 10.1056/nejm198903023200904.
- [45] E. Vieyra-Valdez, R. Linares-Culebro, G. Rosas-Gavilán, D. Ramírez-Hernández, R. Domínguez-Casalá, L. Morales-Ledesma, Roles of the cholinergic system and vagal innervation in the regulation of GnRH secretion and ovulation: experimental evidence, *Brain Res. Bull.* (2020) 129–138, 10.1016/j.brainresbull.2020.09.009.
- [46] J.E. Hall, A.E. Taylor, F.J. Hayes, W.F. Crowley Jr., Insights into hypothalamic-pituitary dysfunction in polycystic ovary syndrome, *J. Endocrinol. Invest.* 9 (1998) 602–611, 10.1007/bf03350785.
- [47] M.W. O'Reilly, A.E. Taylor, N.J. Crabtree, B.A. Hughes, F. Capper, R.K. Crowley, P.M. Stewart, J.W. Tomlinson, W. Arlt, Hyperandrogenemia predicts metabolic phenotype in polycystic ovary syndrome: the utility of serum androstenedione, *J. Clin. Endocrinol. Metab.* 3 (2014) 1027–1036, 10.1210/jc.2013-3399.
- [48] R. Pasquali, V. Vicennati, A. Gambineri, U. Pagotto, Sex-dependent role of glucocorticoids and androgens in the pathophysiology of human obesity, *Int. J. Obes.* 12 (2008) 1764–1779, 10.1038/ijo.2008.129.
- [49] S. Rajaei, Ph D.A. Alihemmati, Ph D.A. Abedelahi, Antioxidant effect of genistein on ovarian tissue morphology, oxidant and antioxidant activity in rats with induced polycystic ovary syndrome, *Int. J. Reprod. Biomed.* 1 (2019) 11–22, 10.18502/ijrm.v17i1.3816.
- [50] E. Diamanti-Kandarakis, A. Dunaif, Insulin resistance and the polycystic ovary syndrome revisited: an update on mechanisms and implications, *Endocr. Rev.* 6 (2012) 981–1030, 10.1210/er.2011-1034.
- [51] F.K.H. Shirazi, Z. Khodamoradi, M. Jeddi, Insulin resistance and high molecular weight adiponectin in obese and non-obese patients with Polycystic Ovarian Syndrome (PCOS), *BMC Endocr. Disord.* 1 (2021) 45, 10.1186/s12902-021-00710-z.
- [52] S. Shorakae, S. Ranasinha, S. Abell, G. Lambert, E. Lambert, B. de Courten, H. Teede, Inter-related effects of insulin resistance, hyperandrogenism, sympathetic dysfunction and chronic inflammation in PCOS, *Clin. Endocrinol.* 5 (2018) 628–633, 10.1111/cen.13808.
- [53] Y. Xu, J. Qiao, Association of insulin resistance and elevated androgen levels with polycystic ovarian syndrome (PCOS): a review of literature, *J. Healthc. Eng.* (2022), 9240569, 10.1155/2022/9240569.
- [54] A.K. Schröder, S. Tauchert, O. Ortman, K. Diedrich, J.M. Weiss, Insulin resistance in patients with polycystic ovary syndrome, *Ann. Med.* 6 (2004) 426–439, 10.1080/07853890410035296.
- [55] D.E. James, J. Stöckli, M.J. Birnbaum, The aetiology and molecular landscape of insulin resistance, *Nat. Rev. Mol. Cell Biol.* 11 (2021) 751–771, 10.1038/s41580-021-00390-6.
- [56] M. Soltani, M. Moghimian, S.H. Abtahi-Evari, S.A. Esmaeili, R. Mahdipour, M. Shokoohi, The effects of clove oil on the biochemical and histological parameters, and autophagy markers in polycystic ovary syndrome-model rats, *International journal of fertility & sterility* 3 (2023) 187–194, 10.22074/ijfs.2022.543640.1260.
- [57] J. Nawrocka-Rutkowska, I. Szydłowska, K. Jakubowska, M. Olszewska, D. Chlubek, M. Szczuko, A. Starczewski, The role of oxidative stress in the risk of cardiovascular disease and identification of risk factors using AIP and castelli atherogenicity indicators in patients with PCOS, *Biomedicines* 7 (2022), 10.3390/biomedicines10071700.
- [58] M. Mohammadi, Oxidative stress and polycystic ovary syndrome: a brief review, *Int. J. Prev. Med.* 86 (2019), 10.4103/ijpvm.IJPVM_576_17.
- [59] N. Peker, G. Turan, S. Ege, M.H. Bademkuran, T. Karaçor, Ö. Erel, The effect of clomiphene citrate on oxidative stress parameters in polycystic ovarian syndrome, *J. Obstet. Gynaecol. : the journal of the Institute of Obstetrics and Gynaecology* 1 (2021) 112–117, 10.1080/01443615.2020.1719052.
- [60] F. Gharanjik, M.B. Shojaeifard, N. Karbalaeei, M. Nemati, The effect of hydroalcoholic calendula officinalis extract on androgen-induced polycystic ovary syndrome model in female rat, *BioMed Res. Int.* (2022), 7402598, 10.1155/2022/7402598.
- [61] K.M. Hoeger, S.E. Oberfield, Do women with PCOS have a unique predisposition to obesity? *Fertil. Steril.* 1 (2012) 13–17, 10.1016/j.fertnstert.2011.11.026.
- [62] B. Yildirim, S. Demir, I. Temur, R. Erdemir, B. Kaleli, Lipid peroxidation in follicular fluid of women with polycystic ovary syndrome during assisted reproduction cycles, *J. Reprod. Med.* 8 (2007) 722–726.
- [63] D. Wang, Y. Weng, Y. Zhang, R. Wang, T. Wang, J. Zhou, S. Shen, H. Wang, Y. Wang, Exposure to hyperandrogen drives ovarian dysfunction and fibrosis by activating the NLRP3 inflammasome in mice, *Sci. Total Environ.* (2020), 141049, 10.1016/j.scitotenv.2020.141049.
- [64] O.M.S. Niño, C.S. da Costa, K.M. Torres, J.F. Zanol, L.C. Freitas-Lima, L. Miranda-Alves, J.B. Graceli, High-refined carbohydrate diet leads to polycystic ovary syndrome-like features and reduced ovarian reserve in female rats, *Toxicol. Lett.* (2020) 42–55, 10.1016/j.toxlet.2020.07.002.
- [65] L.C. McIlvenna, R.K. Patten, A.J. McAinch, R.J. Rodgers, N.K. Stepto, A. Moreno-Asso, Transforming growth factor beta 1 alters glucose uptake but not insulin signalling in human primary myotubes from women with and without polycystic ovary syndrome, *Front. Endocrinol.* (2021), 732338, 10.3389/fendo.2021.732338.
- [66] L. Chen, T. Yang, D.W. Lu, H. Zhao, Y.L. Feng, H. Chen, D.Q. Chen, N.D. Vaziri, Y.Y. Zhao, Central role of dysregulation of TGF-β/Smad in CKD progression and potential targets of its treatment, *Biomed. Pharmacother.* (2018) 670–681, 10.1016/j.biopha.2018.02.090.
- [67] K.L. Walton, K.E. Johnson, C.A. Harrison, Targeting TGF-β mediated SMAD signaling for the prevention of fibrosis, *Front. Pharmacol.* (2017) 461, 10.3389/fphar.2017.00461.
- [68] E.G. El-Waseif, M.H. Sharawy, G.M. Suddek, The modulatory effect of sodium molybdate against cisplatin-induced CKD: role of TGF-β/Smad signaling pathway, *Life Sci.* (2022), 120845, 10.1016/j.lfs.2022.120845.
- [69] M.J. Hao, P.N. Chen, H.J. Li, F. Wu, G.Y. Zhang, Z.Z. Shao, X.P. Liu, W.Z. Ma, J. Xu, T. Mahmud, W.J. Lan, β-Carboline alkaloids from the deep-sea fungus *Trichoderma* sp. MCCC 3A01244 as a new type of anti-pulmonary fibrosis agent that inhibits TGF-β/smad signaling pathway, *Front. Microbiol.* (2022), 947226, 10.3389/fmicb.2022.947226.
- [70] A. Ma, F. Zou, R. Zhang, X. Zhao, The effects and underlying mechanisms of medicine and food homologous flowers on the prevention and treatment of related diseases, *J. Food Biochem.* 12 (2022), e14430, 10.1111/jfbc.14430.
- [71] Z.L. Miao, L. Guo, Y.X. Wang, R. Cui, N. Yang, M.Q. Huang, W.B. Qin, J. Chen, H.M. Li, Z.N. Wang, X.C. Wei, The intervention effect of Rosiglitazone in ovarian fibrosis of PCOS rats, *Biomed. Environ. Sci.* 1 (2012) 46–52, 10.3967/0895-3988.2012.01.007.
- [72] D.H. Assar, A.A. Mokhbatly, E.W. Ghazy, Z.I. Elbially, A.A. Gaber, A.A. Hassan, A. Nabil, S.A. Asa, Silver nanoparticles induced hepatotoxicity via the apoptotic/antiapoptotic pathway with activation of TGFβ-1 and α-SMA triggered liver fibrosis in Sprague Dawley rats, *Environ. Sci. Pollut. Res. Int.* 29 (2022) 80448–80465, <https://doi.org/10.1007/s11356-022-21388-3>.